

МИНИСТЕРСТВО ЭНЕРГЕТИКИ РЕСПУБЛИКИ КАЗАХСТАН
АКЦИОНЕРНОЕ ОБЩЕСТВО «НАЦИОНАЛЬНАЯ АТОМНАЯ КОМПАНИЯ «КАЗАТОМПРОМ»
АО «ВОЛКОВГЕОЛОГИЯ»



СБОРНИК ТРУДОВ

IX МЕЖДУНАРОДНОЙ НАУЧНО-ПРАКТИЧЕСКОЙ КОНФЕРЕНЦИИ

АКТУАЛЬНЫЕ ПРОБЛЕМЫ УРАНОВОЙ ПРОМЫШЛЕННОСТИ

7-9 ноября 2019, г. Алматы, Республика Казахстан



KAZATOMPROM
NATIONAL ATOMIC COMPANY



АО «НАЦИОНАЛЬНАЯ АТОМНАЯ КОМПАНИЯ «КАЗАТОМПРОМ»
АО «ВОЛКОВГЕОЛОГИЯ»



СБОРНИК ТРУДОВ
IX МЕЖДУНАРОДНОЙ НАУЧНО-ПРАКТИЧЕСКОЙ КОНФЕРЕНЦИИ

АКТУАЛЬНЫЕ ПРОБЛЕМЫ УРАНОВОЙ ПРОМЫШЛЕННОСТИ

7 - 9 ноября 2019 года

Часть 1

Алматы
2019

STOCHASTIC MODELING OF ROLLFRONT URANIUM DEPOSIT BASED ON REACTIVE TRANSPORT AND STREAMLINE SIMULATION

*Aizhulov D.Y., Shayakhmetov N.M., Kurmanseit M.B.,
Tungatarova M.S., Kaltayev A.*

Satbayev University, Almaty, Kazakhstan

Since the process of formation of rollfront type uranium deposits is very specific from the point of view of hydrodynamics and chemical kinetics, studies were conducted to create a model for the genesis of such mineralization (published in [2]). The genesis of rollfront type deposits comprises three main stages (Figure 1): leaching phase by oxygenated water, migration of the diluted chemical components and lastly deposition of minerals. In the case of the Tianshian mega-province, southern Kazakhstan, which hosts as much as 1.400 Mt of uranium, oxygen rich rainwater leached uranium-enriched minerals including zircons, monazites, and accessory minerals, from the granitic Tianshian Mountains, and then transported it downstream through the unconsolidated porous sandstones. Later on, when reaching reduced environments, the dissolved uranium together with other elements such as iron and sulfurs precipitated as uranium minerals (mainly pitchblende and coffinite in the Kazakhstan uranium deposits) and pyrite (FeS_2), thereby forming a rollfront type deposit. It is important to note, that the re-deposition of minerals is a dynamic dissolving/precipitation process sustained by a continuous flow of oxygenated meteoritic water which push minerals further downstream. In other words, in active deposits, minerals continuously dissolve from the upstream side of the mineralization zone and precipitate at the front side rear. When no more oxygen is available in the water flow, often because it has been consummated previously by the oxidation of the organic matter before reaching the mineralized zone, the rollfront stabilize [3].

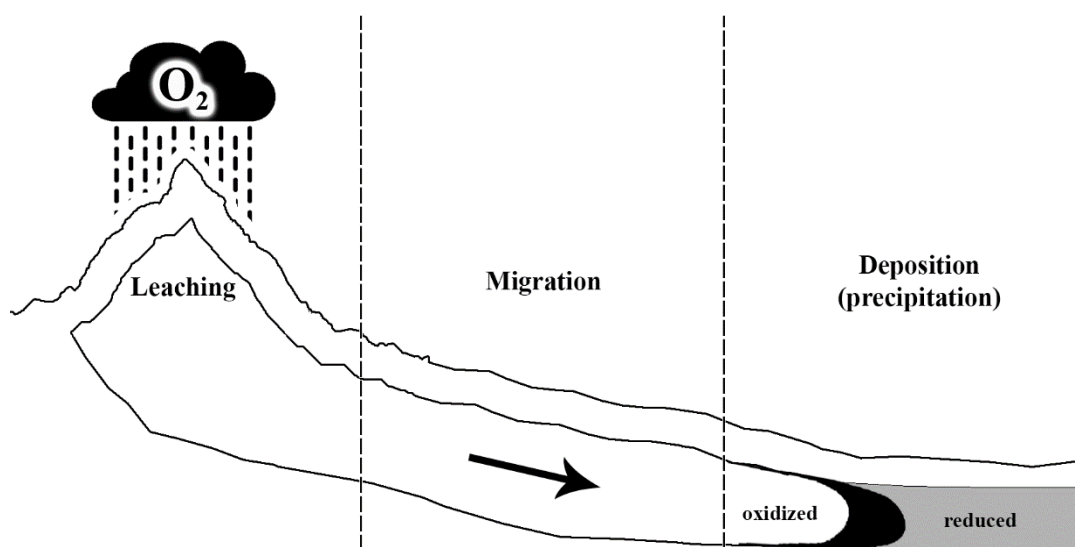


Figure 1 – Stages of rollfront uranium deposit formation

The formation of uranium deposits involves complex kinetics of various compounds described in the literature [4, 5].

Evseeva et al. [6] conducted a dissolution/precipitation experiment in which she managed to mimic the formation of the uranium rollfront deposits in laboratory conditions. The experimental results were compared with the numerical results of the model by reproducing the experiment conditions. Evseeva used a transparent plastic box ($2 \times 0.15 \times 0.2$ m) filled with sand (Figure 2). After several chemical manipulations, the iron oxide contained in the box was converted to sulfides

thereby creating a reduced environment. A water containing uranium concentration (around 10^{-6} - 10^{-5} g·l⁻¹ gram per liter) was flowed through the box leading to the formation of a roll-like accumulation of uranium in the box.

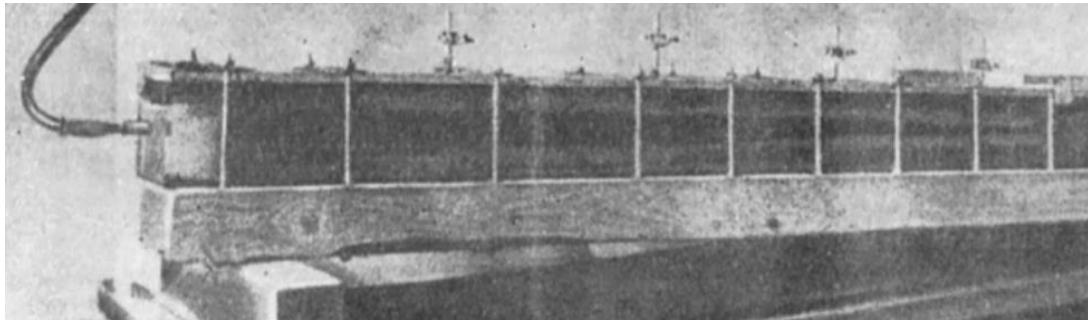


Figure 2 – Laboratory experiment conducted by Evseeva to simulate genesis of rollfront uranium deposit

The resulting distribution of the uranium in the box is due to a stable increase in uranium concentration and the shifting of the oxidation zone into the reduced sands. When the experiment was conducted, showing that the above-mentioned laboratory experiment reproduces quite well the roll-like accumulations of uranium, there was no satisfactory explanations on the mechanisms responsible for the occurrence of such shapes.

Since rollfront deposits form in porous medium, as underlined by Goldshtik M. A. [7], a definitive diffusive extension of a deposit “tongue” (or uranium wings) cannot be explained by not considering a slip boundary conditions for the viscous flow. Other factors must be responsible for the formation of the crescent shaped mineralization.

During the numerical experimentation conducted by the authors rollfront genesis mechanisms were determined together with reasons for its distinctive crescent shape.

Several assumptions were made in the context of the experiment:

1. the fluids in the box are incompressible, and the flow of reagents occur in the water;
2. in comparison with convective transfer, the diffusion transport of the mineral is much lower;
3. the amount of reductant is much higher than of other reagents;
4. the concentration of oxidant used in the experiment were as low as 0.001 g·l⁻¹ which would
5. be close to the groundwater oxygen concentrations in Central Asia deposits.

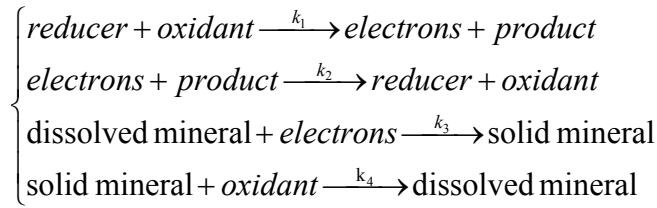
The medium under consideration is porous and permeable, while the Darcy equation is a time-tested instrument to simulate underground fluid flow in porous medium:

$$\operatorname{div} \vec{u} = 0$$

$$\vec{u} = -\frac{K}{\mu} \operatorname{grad} p$$

where the first equation describes the mass conservation, whereas the second one defines the flow velocity in the porous medium.

Based on the Law of Mass Action [8] and aforementioned principles of rollfront formation and laboratory experiment following scenario was simulated by numerical experiment. Into the box containing porous medium with high concentration of a reductant C_{red} , a constant inflow of water with concentrations of dissolved uranium C_{dis} and oxidant C_{ox} was imposed through inlet over a period of 60 days. Redox reaction between reductant and oxidant are simplified by the following scheme:



Notations and definitions used to construct the model a listed in the following table.

Table 1 - Notations and definitions used in the model of rollfront formation

Notation	Definition
C_{dis}	dissolved mineral concentration ($\text{g}\cdot\text{l}^{-1}$)
C_{sol}	solid (precipitated) mineral concentration ($\text{g}\cdot\text{l}^{-1}$)
C_{red}	reduced environment concentration ($\text{g}\cdot\text{l}^{-1}$)
C_{ox}	oxidizer concentration ($\text{g}\cdot\text{l}^{-1}$);
C_e	electron bearing elements concentration ($\text{g}\cdot\text{l}^{-1}$);
C_{pr}	product of reductant oxidation concertation ($\text{g}\cdot\text{l}^{-1}$)
$k_i, i = \overline{1,4}$	reaction constant for each reaction
ρ	total density ($\text{kg}\cdot\text{m}^{-3}$)
ρ_{liquid}	liquids density ($\text{kg}\cdot\text{m}^{-3}$);
ρ_{solid}	solids density ($\text{kg}\cdot\text{m}^{-3}$)
K	permeability (m^2)
$\vec{u} = \{u_x, u_y\}$	flow velocity ($\text{m}\cdot\text{sec}^{-1}$) with its components by x and y axes
μ	viscosity ($\text{Pa}\cdot\text{sec}$)
p	pressure (Pa)
t	time (sec)
θ	porosity

The model of formation of uranium deposits is described by the following system of differential equations:

$$\begin{aligned} \frac{\partial C_{red}}{\partial t} &= \frac{k_2 C_e C_{pr} - k_1 C_{red} C_{ox}}{(1-\theta)\rho_{solid}} \\ \frac{\partial C_{ox}}{\partial t} + \vec{u} \cdot \text{grad} C_{ox} &= \frac{k_2 C_e C_{pr} - k_1 C_{red} C_{ox} - k_4 C_{sol} C_{ox}}{\theta\rho_{liquid}} \\ \frac{\partial C_{pr}}{\partial t} + \vec{u} \cdot \text{grad} C_{pr} &= \frac{k_1 C_{red} C_{ox} - k_2 C_e C_{pr}}{\theta\rho_{liquid}} \\ \frac{\partial C_{pr}}{\partial t} + \vec{u} \cdot \text{grad} C_{pr} &= \frac{k_1 C_{red} C_{ox} - k_2 C_e C_{pr}}{\theta\rho_{liquid}} \\ \frac{\partial C_e}{\partial t} + \vec{u} \cdot \text{grad} C_e &= \frac{k_1 C_{red} C_{ox} - k_2 C_e C_{pr} - k_3 C_e C_{dis}}{\theta\rho_{liquid}} \end{aligned}$$

$$\frac{\partial C_{dis}}{\partial t} + \rho \cdot \mathit{grad} C_{dis} = \frac{k_4 C_{sol} C_{ox} - k_3 C_{dis} C_e}{\theta \rho_{liquid}}$$

$$\frac{\partial C_{sol}}{\partial t} = \frac{k_3 C_e C_{dis} - k_4 C_{sol} C_{ox}}{(1-\theta) \rho_{solid}}$$

Boundary conditions used in numerical experiment were similar to those of the laboratory experiment. According to the experiment Evseeva et al. [6], atmospheric pressure boundary condition is imposed at the outlet

$$p|_{outlet} = p_{atm}$$

while a constant boundary condition is imposed to the flow velocity at $1.44 \cdot 10^{-4} \text{ m}\cdot\text{s}^{-1}$ at the inlet, which corresponds to

$$p|_{inlet} = p_{atm} + \rho gh$$

with h equal to 0.74 meters. Apart from inlet and outlet no-flow boundary condition is imposed to all solid sides of the box

$$\rho \cdot \mathit{grad} p|_{sides} = 0 \text{ or } \frac{\partial p}{\partial n}|_{sides} = 0$$

Other boundary conditions for all concentrations in liquid phase, conform to following boundary conditions (measured in gram per liter):

$$C_{dis}|_{inlet} = 7.5 \cdot 10^{-5}, C_{ox}|_{inlet} = 0.002, C_e|_{inlet} = 0, C_{pr}|_{inlet} = 0$$

$$\frac{\partial^2 C_{dis}}{\partial n^2}|_{outlet} = 0, \frac{\partial^2 C_{ox}}{\partial n^2}|_{outlet} = 0, \frac{\partial^2 C_e}{\partial n^2}|_{outlet} = 0, \frac{\partial^2 C_{pr}}{\partial n^2}|_{outlet} = 0$$

$$\frac{\partial C_{dis}}{\partial n}|_{sides} = 0, \frac{\partial C_{ox}}{\partial n}|_{sides} = 0, \frac{\partial C_e}{\partial n}|_{sides} = 0, \frac{\partial C_{pr}}{\partial n}|_{sides} = 0$$

The initial conditions for the concentrations of liquids are:

$$C_{dis}|_{t=0} = 0, C_{ox}|_{t=0} = 0, C_e|_{t=0} = 0, C_{pr}|_{t=0} = 0$$

The initial conditions for the concentrations of solids are:

$$C_{sol}|_{t=0} = 0, C_{red}|_{t=0} = 1$$

Before the inflow started, there was no uranium in the box, and it was filled with the reduced porous medium (sand + ferrous iron).

According to this model, the solid uranium can only form by a precipitation reaction only. An analytical solution to the set of the considered differential equations given the above boundary and initial conditions is quite difficult to achieve; thus they were solved numerically using the COMSOL Multiphysics software.

Upon conforming with the laboratory experiment, numerical simulation was further extended while crescent shaped rollfront redistributed concentrations were observed in the numerical simulation as illustrated on Figure 3 over a period of 3,300 days with an inflow velocity at $10^{-4} \text{ m}\cdot\text{s}^{-1}$; in these conditions, the deposit moved over a distance of about 15 meters conserving its shape.

The rollfront is gradually shifted over time along the stream flow (Figure A.27), despite of the absence of the convection or diffusion terms in the solid uranium concentration equation. Hence, this shift is a result of the dissolution/precipitation chemical reactions. The reducer is leached and

redeposited together with the uranium minerals while some of its concentration is consumed in order to reduce the dissolved uranium.

One should note that a small hose is observed in the velocity field near the inflow point both in the laboratory and in the numerical experiment. The non-parallel flow at the inlet is probably at the origin of the crescent shape observed in the uranium deposition, the flow being higher in the middle of the box than on the edges (no uniform inlet flow). Then, the flow stabilizes into a parallel flow regime for greater distances, indicating that this is not the viscosity of the fluid which is at the origin of the slowdown of the flow along the inlet edges. To test this assumption, the boundary conditions were redesigned without this narrowing in the inflow. The recalculation gives a results with a straight front. Therefore, the rollfront shape would result in a non-homogeneously distributed inlet velocity flow. Therefore, these numerical tests suggest that it that the roll-like shapes forms due to a squeeze (or constriction) of the channel in which the flow occurs, and consequently increase the flow velocity, and thus to a subsequent change in the pressure gradient. Further numerical experiments were conducted with various channel constrictions (Figure 4). Various geometries with widening (Figure 4), and constricting and expanding channels (Figure 4), were numerically simulated both for the pressure field, and for the solid mineral concentration. All these cases exhibit a crescent like shape front. Even after the pressure distribution straightens, the concentration front does not recover its original shape. This can be explained by the fact that in the experiment, the concentration of oxygen probably was too low to redeposit substantial amounts of mineral further to the right during such a short period.

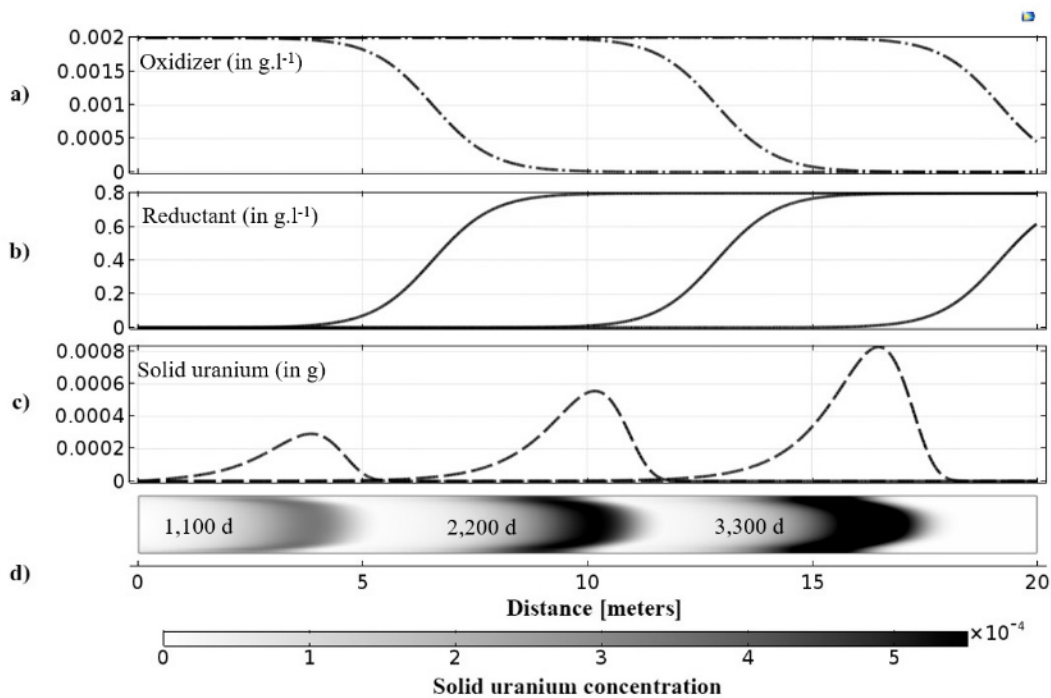


Figure 3 – Re-deposition of uranium over the periods of 1,100, 2,200, and 3,300 days, respectively. a) Oxidizer concentration; b) Reductant concentration; c) Solid uranium concentration. d) Solid uranium concentration in 2D

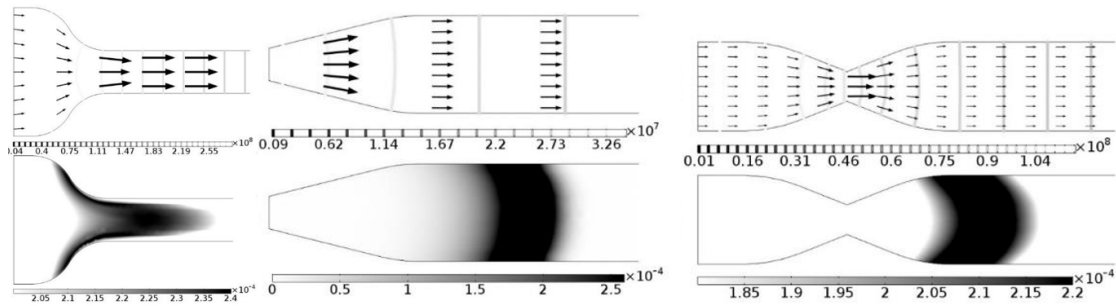


Figure 4 – Resulting solid mineral concentration with the typical crescent like shape for the rollfront. Lines represent flow velocity. Crescent shape resulting from expansion of the channel.
Crescent shaped rollfront after constriction and expansion of the channel

Thus, the model of rollfront uranium deposit formation not only shows the high role of hydrodynamics in the process of its genesis, but also provided the ability to create synthetic deposits for verification of stochastic methods. Synthetic deposits are very useful due to the closeness of the uranium industry, and since the actual distribution of underground mineralization is usually not known even after decommissioning. Real concentration is known only along wells based on well log data.

Since hydrodynamics played an important role in the formation of rollfront deposits, the authors carried out work to create a new method of geostatistics based on streamlines [9].

One of the main difficulties in the exploration of uranium rollfront type deposits lies in the limited number of available exploration techniques that, at small scale, are generally limited to the drilling of numerous costly wells network patterns in perspective areas [10], which in itself is a long and costly process. The goal of interpolation techniques is to determine the geometry and content of the deposit in inter-well space based on well log data.

In various geostatistical estimation methods such as inverse distance method or method of Kriging, weight is assigned to hard data based on the distance to the node under consideration. Two basic approaches to modeling exist at the moment: the traditional interpretation of geophysical data with the subsequent connection of ore contours; and geostatistical 3D modeling [11]. Presently, there are a number of stochastic methods for modeling rollfront uranium deposits by Renard D., Beucher H. [12], Petit et al [13] and Abzalov et al. Renard D. and Busher G. V, developed the technology of three-dimensional modeling of such deposits based on the model of "PluriGaussian Simulation". Unfortunately, current modeling techniques rarely account for the hydrodynamic and geochemical processes involved in the genesis of rollfront uranium deposits. The authors propose to supplement existing stochastic models with additional methods of computational hydrodynamics. Approach used in this work is based on calculating streamlines, which are a family of curves that are instantaneously tangent to the velocity vector of the flow. Streamlines show the direction in which a massless fluid element will travel at any point in time. Time of flight is the time that such an object needs to travel a distance through a medium.

Application of various estimation methods such as inverse distance weighting or kriging are based on weight assignment to well data in order to determine value at any specific node on a computational grid. Value $Z^*(x)$ at node x is dependent on each hard data node x_i and the weight λ_i assigned to it:

$$Z^*(x) = \sum_{i=1}^n \lambda_i Z(x_i)$$

Weight assignment technique is a determining factor that differentiates one estimation algorithm from another. For instance, while in kriging based methods, variogram is used for weight computation, in inverse distance based methods (as the name suggests) the length of space between nodes is main influencing factor.

Streamline based Kriging interpolation consists of following steps: calculate pressure field based on filtration properties from hard data; calculate velocity field based on Darcy Law; calculate streamlines; calculate time of flight along the streamline; substitute distances with time of flight for Kriging calculations; continue calculation using conventional kriging algorithm.

In many implementations of kriging, search ellipsoid is used to gather input information from well log data. The form of this ellipsoid is usually dictated by anisotropy of a particular geological formation. In current work, based on filtration properties gathered from well data and natural head difference, streamlines of solution flow through stratum under consideration were determined. These streamlines were further used as a search shape for distance based methods, while variograms were calculated along the streamline by substituting distance variable with “time of flight” (a property specific to streamline simulation methods). A search radius that is usually used in kriging implementations is used for streamline based kriging implementations. However, in our case a collection of search radiuses is used along the streamline, that pass through nodes under consideration to collect hard data and assign appropriate weights.

Variogram is calculated over each streamline using time of flight instead of distance:

$$\gamma(h) = \frac{1}{N(h)} \sum_{N(h)} E[Z(\tau(x) + h) - Z(\tau(x))]^2$$

where $\gamma(h)$ is a variogram at the distance h , $N(h)$ is a number of nodes separated by distance h , $\tau(x)$ is a time of flight of node x over a streamline that passes through it.

Weights are determined for each hard data node found along the streamline:

$$\lambda_i = \frac{C(\tau(x_i))}{\sum_{j=1}^n C(\tau(x_j))}$$

where C is a covariogram calculated as $C(h) = \sigma^2 - \gamma(h)$.

To verify the stochastic modeling approach of uranium rollfront deposits based on streamline simulation, well log data from Kazakhstan deposits were used. In each verification iteration one or more well data were excluded from modeling input for later comparison between numerical and hard data. For further verification purposes, synthetic deposits were simulated based on reactive transport models by reproducing involved uranium rollfront deposit formation. Results were compared with conventional kriging algorithm implemented in SGeMS software. The work was supported by the Ministry of Education of Kazakhstan through the program of targeted financing BR05236447.

1. Strata Geo software for building a 3D geological model of uranium deposits from well data: certificate of authorship 004542 Kazakhstan / A. Kaltayev, M.S. Tungatarova, A.B Kuljabekov, M.B. Kurmanseit, A.B. Koldas, D.Y. Aizhulov; authors are applicant and copyright holder. – №0942/16; stated 11.03.16; published 20.05.16. – 1 p. (russian)

2. Regnault, O. 3D reactive transport simulations of uranium in situ leaching. Forecast and process optimization for increasing technological blocks performance / O. Regnault, N. Fiet, V. Lagneau, R. Mathieu, V. Garnier, V. Selezneva, A. Pouradier, S. Petiteau // Actual problems of the uranium industry: a collection of works of scientific-practical conference. – Astana: Publishing house of JSC National atomic company Kazatomprom, 2014. – pp. 65-68.

3. Dahlkamp, F.J. Uranium deposits of the world: Asia / F.J. Dahlkamp. – Berlin.: Springer-Verlag, 2009. – 492 p.
4. Romberger, S.B. Transport and deposition of uranium in hydrothermal systems at temperatures up to 300C: geological implications / S.B. Romberger // Uranium geochemistry, mineralogy, geology, exploration and resources. – 1984. – pp. 12-17.
5. Maksimova, M.F. Rollfront ore formation / M.F. Maksimova, Y.M. Shmariovich. – Moscow: Nedra, 1993. – 160 p.
6. Evseeva, L.S. Some laws of the formation of epigenetic uranium ores in sandstones, derived from experimental and radiochemical data / L.S. Evseeva, K.E. Ivanov, V.I. Kochetkov // Atomnaya energiya. – 1962. – № 14. – pp. 474-481.
7. Goldshtik, M.A. Transfer processes in the granular layer / M.A. Goldshtik. – Novosibirsk: Publishing house of Teplophysics Institute Siberian Branch of the Russian Academy of Sciences, 1984. – 163 p. (russian)
8. Danayev, N.T. Mass transfer in the near-well zone and electromagnetic logging / N.T. Danayev, N.K. Korsakova, V.I. Penkovsky. – Almaty: Kazakh university, 2005. – 180 p. (russian)
9. Aizhulov, D.E. Stochastic modelling of uranium roll-front deposits based on streamline simulation / D.E. Aizhulov, A. Kaltayev // International symposium on uranium raw material for the nuclear fuel cycle: exploration, mining, production, supply and demand, economics and environmental issues (URAM-2018). – Vienna: IAEA, 2018. – pp. 17-20.
10. Brovin, K.G. Forecast, prospecting, exploration and industrial evaluation of uranium deposits for mining by in-situ leaching / K.G. Brovin, V.A. Grabovnikov, M.V. Shumilin, V.G. Yazikov. – Almaty: Gylym, 1997. – 384 p. (russian)
11. Abzalov, M. Resource estimation of in situ leach uranium projects / M. Abzalov, S. Drobov, O. Gorbatenko, A. Vershkov, O. Bertoli, D. Renard, H. Beucher // Transactions of the Institution of Mining and Metallurgy. – 2014. – Vol. 123. – № 2. – pp. 70-85.
12. Renard, D. 3D representations of a uranium roll-front deposit / D. Renard, H. Beucher // Transactions of the Institution of Mining and Metallurgy. – 2012. – Vol. 121. – № 2. – pp. 84-88.
13. Petit, G. Application of Stochastic Simulations and Quantifying Uncertainties in the Drilling of Roll Front Uranium Deposits / G. Petit, H. Boissezon, V. Langlais, G. Rumbach, A. Khairuldin, T. Oppeneau, N. Fiet // Quantitative Geology and Geostatistics. – 2012. – Vol 17. – pp. 321-332.

СОДЕРЖАНИЕ

Приветственное слово	I
----------------------------	---

РАЗДЕЛ I. РАСШИРЕНИЕ И УКРЕПЛЕНИЕ УРАНОВОЙ МИНЕРАЛЬНО-СЫРЬЕВОЙ БАЗЫ, СОВРЕМЕННЫХ МЕТОДОВ ЕЕ ПРОГНОЗИРОВАНИЯ И РАЗВЕДКИ

<i>Романов А.М.</i> ПРИМЕНИМОСТЬ ГЕОФИЗИЧЕСКИХ МЕТОДОВ ДЛЯ ВЫДЕЛЕНИЯ СТРУКТУР, ПЕРСПЕКТИВНЫХ НА ОБНАРУЖЕНИЕ УРАНОВОГО ОРУДЕНЕНИЯ.....	3
<i>Пахомов В.И., Дуйсебаев Б.О.</i> МЕТОДОЛОГИЯ СИСТЕМНОГО ЦЕЛЕВОГО ПРОГНОЗА (СЦП) МЕСТОРОЖДЕНИЙ ПОЛЕЗНЫХ ИСКОПАЕМЫХ. (НА ПРИМЕРЕ ПОИСКОВ УРАНОВЫХ МЕСТОРОЖДЕНИЙ) ..	13
<i>Машиковцев Г.А.</i> ПЕРСПЕКТИВЫ РАЗВИТИЯ МИНЕРАЛЬНО-СЫРЬЕВОЙ БАЗЫ УРАНА РОССИИ И СОВРЕМЕННЫЕ ПОИСКОВЫЕ ТЕХНОЛОГИИ.....	19
<i>Волобуев Г.Т., Домаренко В.А.</i> ТОРИЙ ЕНИСЕЙСКОГО КРЯЖА И ЕГО ЗНАЧЕНИЕ В АТОМНОМ ПРОЕКТЕ СССР	23
<i>Вершков А.Ф., Мирзагелдиев Е.О., Сейтимбетова Г.К., Арустамов А.А.</i> СОВРЕМЕННЫЕ ВОЗМОЖНОСТИ ИССЛЕДОВАНИЯ ГОРНЫХ ПОРОД И РУД В ХИМИКО-АНАЛИТИЧЕСКОЙ ЛАБОРАТОРИИ ФИЛИАЛА ЦОМЭ АО «ВОЛКОВГЕОЛОГИЯ».....	30
<i>Мендыгалиев А.А., Вершков А.Ф., Джартыбаев Н.Б.</i> РАЗВИТИЕ И ВОСПОЛНЕНИЕ МИНЕРАЛЬНО-СЫРЬЕВОЙ БАЗЫ УРАНА КАЗАХСТАНА ДЛЯ ОБЕСПЕЧЕНИЯ ДОЛГОСРОЧНЫХ ПОТРЕБНОСТЕЙ УРАНОВОЙ ОТРАСЛИ РЕСПУБЛИКИ КАЗАХСТАН	31
<i>Поцелуев А.А., Рихванов Л.П.</i> КОМПЛЕКСНЫЙ СОСТАВ РУД СЕВЕРО-КАЗАХСТАНСКОЙ УРАНОВОРУДНОЙ ПРОВИНЦИИ	35
<i>Aizhulov D.Y., Shayakhmetov N.M., Kurmanseit M.B., Tungatarova M.S., Kaltayev A.</i> STOCHASTIC MODELING OF ROLLFRONT URANIUM DEPOSIT BASED ON REACTIVE TRANSPORT AND STREAMLINE SIMULATION	47
<i>Мухамедяров Р.Д., Дабаев А.И., Антипов С.М.</i> ИНТЕГРАЦИЯ КОСМИЧЕСКИХ И НАЗЕМНЫХ МЕТОДОВ РАЗВЕДКИ – ЭФФЕКТИВНЫЙ СПОСОБ ИЗУЧЕНИЯ ПЕРСПЕКТИВ УРАНОНОСНОСТИ, ПОИСКА И РАЗВЕДКИ МЕСТОРОЖДЕНИЙ УРАНА	55
<i>Домаренко В.А.</i> КОНЦЕПЦИЯ РАЗВИТИЯ ПРОГНОЗНЫХ И ПОИСКОВЫХ РАБОТ НА УРАН В СРЕДНЕЙ СИБИРИ	64
<i>Карчевский И.Е., Першин М.Е.</i> ГЕОТЕХНОЛОГИЧЕСКАЯ ОЦЕНКА ПОЛНОТЫ ОТРАБОТКИ ПРОМЫШЛЕННЫХ ЗАПАСОВ СРЕДСТВАМИ СОПРЯЖЕННОГО ТРЕХМЕРНОГО И ГИДРОДИНАМИЧЕСКОГО МОДЕЛИРОВАНИЯ НА ОСНОВЕ ЭПИГНОЗНОГО АНАЛИЗА ФАКТИЧЕСКИ ДОСТИГНУТЫХ ПОКАЗАТЕЛЕЙ.....	72
<i>Петровский В.Б., Карелин В.Г.</i> К МЕТОДИКЕ ПОИСКОВ ПЛАСТОВО-ИНФИЛЬТРАЦИОННЫХ И ПАЛЕОРУСЛОВЫХ МЕСТОРОЖДЕНИЙ УРАНА НА ОСНОВЕ ПРИМЕНЕНИЯ ИННОВАЦИОННЫХ МЕТОДОВ... ..	73
<i>Толмачев С.И.</i> ИСТОРИЯ ОТРАСЛИ. ВЗГЛЯД ЧЕРЕЗ ИННОВАЦИИ	80